

General Disclaimer

One or more of the Following Statements may affect this Document

- This document has been reproduced from the best copy furnished by the organizational source. It is being released in the interest of making available as much information as possible.
- This document may contain data, which exceeds the sheet parameters. It was furnished in this condition by the organizational source and is the best copy available.
- This document may contain tone-on-tone or color graphs, charts and/or pictures, which have been reproduced in black and white.
- This document is paginated as submitted by the original source.
- Portions of this document are not fully legible due to the historical nature of some of the material. However, it is the best reproduction available from the original submission.

RADIATIVE INTERACTIONS OF
ELECTRONS WITH MATTER

Final Report

Contract Number: NAS 8-21421

Prepared for George C. Marshall Space Flight Center,
Marshall Space Flight Center, Alabama 35812

by

L. L. Baggerly and C. A. Quarles

Texas Christian University

Fort Worth, Texas 76129

July 1969

N 71-16599

FACILITY FORM 602

(ACCESSION NUMBER)	(THRU)
34	63
(PAGES)	(CODE)
CR-102994	24
(NASA CR OR TMX OR AD NUMBER)	(CATEGORY)

INTRODUCTION

This is the final report of the research work carried out in the radiation physics laboratory at Texas Christian University under NASA Contract NAS 8-21421. The primary purpose of this research is to investigate the fundamental interactions of electrons with matter in the 50 to 150 keV energy range. A central feature of the work is to assemble and test an experiment to measure the differential cross section for bremsstrahlung produced in time coincidence with inelastically scattered electrons.

During the contract period, the research equipment necessary to successfully perform coincidence experiments to study the inelastic interaction of electrons has been procured, assembled and checked out. Preparatory to the actual coincidence measurements, some studies of the total inelastic electron spectrum have been made and these have been a very valuable aid in setting up and checking out the coincidence experiment. It has also been realized that a study of K x-ray production in coincidence with inelastically scattered electrons - the K shell ionization process - is a very important contribution to the inelastic spectrum and should also be studied in detail. The study of the total inelastic spectra and the bremsstrahlung and K ionization coincidence spectra will be continued and extended under NASA contract NAS 8-24658.

In what follows, Section I deals with the experimental equipment that has been developed for the coincidence studies. Section II discusses the experimental work that has been accomplished, outlines the present state of the research effort and indicates where we expect to go next. Section III reviews the graduate and undergraduate student participation in this research work.

I. EXPERIMENTAL EQUIPMENT

1. Electron beam.

The electron beam used in the experimental program is provided by a Texas Nuclear 150 keV Cockcroft-Walton linear accelerator. The accelerator was originally used to accelerate positive ions, but was converted for electrons shortly before NASA support began. The electron source is a hot wire filament and the intensity of the source and the beam is variable over a wide range. The electron beam energy is continuously variable up to the maximum of 150 keV. We have successfully controlled and focussed electron beams from about 50 keV to 150 keV. A schematic layout of the beam transport system is shown in Figure 1.

Under NAS 8-21421, a high voltage ripple filter Model 1151-L2, was purchased from Raytheon Company for use with the accelerator power supply. The filter has been received and tested, but before it can be fully utilized some additional connectors and cables must be purchased and installed. Before installation of the filter, the peak to peak ripple on the high voltage was measured to be 3 percent. At present, the filter can improve this by a factor of about 3. The accelerator power supply is somewhat unusual in that there are two high voltage cables going to the accelerator dome. One cable carries the high voltage and the second cable carries high voltage with 110 volts a.c. superimposed. The difference voltage can thus be used to provide 110 volts a.c. for the filament power supply of the electron gun. The factor of 3 mentioned above is realized when the high voltage output is filtered but the high voltage with 110 volts superimposed is not. When some additional connectors and cables are obtained and installed so that the high voltage can be filtered before the 110 volts a.c. is superimposed, the filter should reduce the ripple by a factor of about 100.

As can be seen in Figure 1, after acceleration to full energy

the beam enters a drift tube where it can be steered and focussed onto a target mounted in the center of the scattering chamber. The beam is steered by two pairs of Helmholtz coils powered by constant current power supplies. The beam is focussed by an electrostatic quadrupole lens. A 1/16 inch aluminum aperture is mounted at the center of the second set of steering coils to collimate the electron beam before focus occurs. The remainder of the drift tube and the scattering chamber is magnetically shielded.

The spot size on the target is presently of the order of 1/32 inch. The position of the spot is usually quite stable over several hours. The beam drift was significantly improved when unregulated power supplies on one pair of Helmholtz coils were replaced with regulated constant current power supplies. The beam drift does become sizeable, however, when a filament is nearing the end of its useful lifetime. A significant beam drift or a large variation in beam intensity is now simply a signal that that filament should be replaced.

The beam spot can be monitored visually when the intensity is sufficient and this visual monitoring facilitates setting up and focussing the beam. The area around the beam collimator and the target can be coated with ZnS which will fluoresce when struck by electrons. A closed circuit T.V. camera is set to look at the beam collimator and a second camera looks at the target through a 135 degree port in the scattering chamber. To obtain a good beam of the desired energy it is necessary to adjust the four power supplies on the steering coils, the quadrupole focus power supply and a focus and extraction voltage on the electron gun itself. Visual monitoring of the beam at the collimator and the target makes it possible to optimize the setting of these various voltages.

In order to make absolute cross section measurements, the beam intensity must be known. The beam intensity can be determined

by trapping the beam in a Faraday cup at the target and then measuring the total charge collected in the Faraday cup. We have felt that it would be very useful to have a continuous monitor of the beam intensity during a data run. Although a Faraday cup placed somewhere behind the target could provide this, it was felt that a Si(Li) electron detector set at a fixed angle to a thin Vyns film mounted ahead of the target would provide a better monitor. This monitor has the distinct advantage of being independent of target material and thickness, and it can be calibrated against the Faraday cup measurement as needed so that absolute cross sections can be determined.

The monitor, at present, consists of a Si(Li) electron detector enclosed in a lead collimator-shield set at about 30 degrees to a thin Vyns film. The film in the beam is mounted just inside the scattering chamber ahead of the target. The detector is permanently mounted below the beam line so it looks at electrons scattered down at 30 degrees to the incident beam. The scattering angle can be adjusted slightly so that the counting rate in the monitor is reasonable for the beam intensity desired. The ratio of monitor counts to collected beam varies from run to run by less than 2%, and this appears adequate as a beam monitor system.

2. Scattering chamber.

The scattering chamber used in the experiment is a twelve inch aluminum chamber constructed at T.C.U. A plan view of the chamber is shown in Figure 2. There are beam entrance and exit ports, and additional ports at ± 90 degrees and 135 degrees to the beam. Electrical connections are made by 4 coaxial vacuum feed-through connectors on the chamber wall. The top is aluminum, can be rotated to any angle, and has a port designed to accept the

Ge(Li) detector cryostat. The bottom of the chamber has a rotatable arm on which an electron detector, collimator and detector cooling device can be mounted. The target holder can be raised and lowered to bring one of three separate targets into the beam line. Both the target position and the angle of the electron detector can be controlled and monitored remotely. The entire chamber is electrically isolated and the target is isolated from the chamber itself.

3. Detectors.

(1) Photon detector

The photon detector used in the experiments is a 5 mm planar lithium drifted germanium Ge(Li) detector. The active area is 80 mm², but this is collimated considerably when in use. The original detector did not meet resolution specifications and was returned to the manufacturer for replacement. The detector we now have has a resolution well within the guaranteed value of 700 ev full width at half maximum (fwhm). Figure 12 shows a portion of a spectrum taken with the present Ge(Li) detector. The peaks are the K_α and K_β characteristic x-rays from a tin target bombarded with 120 keV electrons. The small peak at about 15 keV is a germanium escape peak. The background is predominantly bremsstrahlung from the target. The fwhm of the K_α peak is about 800 ev and the K_α peak is composed of two x-rays: 25.05 keV and 25.57 keV. This is a good indication of the resolution of the system.

The detector cryostat is a gravity feed type with the detector itself mounted behind a 5 mil beryllium window. The first stage of the FET preamplifier is also held at liquid nitrogen temperature. The cryostat is designed to mount in the top of the scattering chamber. A schematic view of the chamber and the Ge(Li) detector is shown in Figure 3. The neck of the cryostat which extends into

the scattering chamber is surrounded by a 1/4 inch brass shield with a hole just in front of the detector window into which brass collimators of various sizes can be inserted.

The efficiency of the full energy peak of the original Ge(Li) detector was measured using the gamma rays and x-rays from calibrated radioactive sources of Ce-139 and Cd-109. It was consistent with what one would expect from a 5 mm thick detector. The efficiency for the present detector will be measured as time permits. It is, of course, necessary to know the detector efficiency in order to make absolute cross section measurements.

A second Ge(Li) detector is now on order from ORTEC. It will also be a 5 mm planar with a 5 mil beryllium window. The cryostat will be the horizontal dipstick type which is easier to handle and has a longer hold time for liquid nitrogen. This detector can be mounted so that it looks at the target through a port in the side of the scattering chamber. It can either be attached to the chamber under vacuum or look through a thin mylar window in the chamber wall. The resolution of this detector should be about 500 eV.

(2) Electron detectors.

The electron detectors are lithium drifted silicon Si(Li) detectors. They are typically 2 mm thick with an active area of 50 to 80 mm². They can be operated at room temperature but the resolution is improved by cooling. The resolution is typically 6-15 keV fwhm depending on the age of the detector, the cleanliness of its surface, and its temperature. When mounted in the scattering chamber, the detectors are cooled by two thermoelectric modules to a temperature of about zero degrees centigrade. This temperature is limited at present by the ratio of the mass of the detector and collimator to be cooled to the mass of the heat sink we can conveniently use.

4. Electronics and Data Handling.

The electronics used in the experiments is fairly conventional. A typical block diagram for a coincidence experiment indicating the various electronic components is shown in Figure 4. Under NAS 8-21421, it has been possible to purchase the necessary additional electronics to give us flexibility in the design of the logic, a much needed backup of important components, and the ability to parallel some important testing operations. We have purchased the following electronic components: ORTEC Model 440A amplifier, ORTEC Model 427 delay amplifier, ORTEC Model 430 scaler, ORTEC Model 420 single channel analyzer, ORTEC Model 414A fast coincidence. In addition we have obtained an updated version of Canberra Model 1441 fast coincidence.

We have designed and built a circuit to start, stop and reset the Canberra scalers, ORTEC scalers, pulse height analyzer and Elcor current integrator. Such a control circuit is very useful in taking data. Because of the different logic requirements of the circuits to be controlled, design and construction of the circuit has been of some educational value for the students as well.

Under NAS 8-21421 we have purchased a magnetic tape readout system for our TMC Model 1001 pulse height analyzer. The unit is a Geoscience Nuclear Model 5110 tape coupler and a Kennedy Model 1600 incremental transport. With this system, we can dump the contents of the pulse height analyzer in blocks of 256, 512 or 1024 six digit words plus one tag word onto computer compatible magnetic tape in a few seconds. The unit writes at 556 bpi. The six digit tag word can be set manually or it will increment automatically as successive records are written on tape.

A machine language subroutine for the IBM 1401 computer has been written to facilitate reading the magnetic tapes. The subroutine resides on the Fortran library tape and can be called from a Fortran IV program. This means that we can do our data analysis

programming Fortran. At present, a program has been written to search the tape for a desired record as indicated by the tag word and list the contents of that record along with the identifying information which is supplied by card input. Other programs to do peak searching, background subtraction, peak integration, etc. will be developed as needed.

5. Targets.

With the Veeco vacuum evaporation system in our laboratory, we have been able to fabricate targets of aluminum and gold in various thicknesses. For the experiments to be described below we made self-supporting aluminum targets in thicknesses of 200 $\mu\text{gm}/\text{cm}^2$ and 400 $\mu\text{gm}/\text{cm}^2$. These thicknesses were determined by using a Cahn Model G-2 electrobalance which was placed in the laboratory by the manufacturer's representative for our evaluation. The precision, reproducibility and ease of use of this balance led us to request permission to purchase one for permanent installation in the lab. The order has been placed and the electrobalance should be delivered in a few weeks. Aluminum targets of about 100 $\mu\text{gm}/\text{cm}^2$ have since been made.

Fabricating targets or, more generally, producing self-supporting thin metallic films by vacuum evaporation and the subsequent lifting of the film onto a target holder is still an art even though the technique is fairly well known. For thin aluminum targets it is sufficient to evaporate a measured amount of aluminum onto a glass slide which has been treated with a light soap solution. The aluminum film is then floated onto distilled water and lifted from the water onto a target holder. The thickness can be determined by weighing the target holder before and after a film of known area is attached. The thickness can also be determined by direct weighing of a second target made simultaneously with the first or, finally by direct weighing of the target itself after it is no longer in use.

Gold targets of the order of $100 \mu\text{gm}/\text{cm}^2$ thickness are difficult to make self-supporting. For these targets, a thin Vyns film is first lifted onto the target holder and the gold is then evaporated directly onto the Vyns film. Vyns is a polyvinyl resin material, manufactured by Dow Chemical Company.

We anticipate also making silver and copper targets. This will give us a nice range of atomic numbers: 13, 29, 47 and 79. For testing purposes, we have also obtained some tin targets ($Z = 50$) from High Voltage Engineering in thicknesses of 40, 80 and $160 \mu\text{gm}/\text{cm}^2$.

II. EXPERIMENTAL PROGRAM

1. Noncoincident inelastic electron spectra.

As part of the program to investigate the electron energy spectrum as a function of scattering angle for electrons produced in coincidence with an inelastic bremsstrahlung photon, we felt that it was necessary to study the noncoincident inelastic electron energy spectrum in some detail. This study has proved to be interesting in itself and has, as anticipated, provided us with information which will be very useful in the coincidence experiments.

The target was aluminum with a thickness of $200 \mu\text{gm}/\text{cm}^2$. The detector was a thermoelectrically cooled 2mm planar Si(Li) electron detector mounted on a moveable arm in the scattering chamber and enclosed in an aluminum collimator and shield. Data was taken at beam energies of 120 keV and 140 keV and scattering angles from 10 degrees to 120 degrees. Not all angles were covered at each energy, however. Our data parallels that of Dick and Motz at 200 and 400 keV.¹ Figures 5 and 6 show data at an incident energy of 120 keV where the most extensive measurements were made. The vertical scale is number of counts and the horizontal scale has been converted

to energy in keV. Each point represents a sum of four channels in the pulse height analyzer.

The most obvious feature in the data is the large peak at the incident energy of 120 keV. This is the Rutherford peak and corresponds to elastic scattering of the electrons from the aluminum atoms. The data at each scattering angle are normalized to this Rutherford peak.

We are interested, of course, in the inelastic portion of the energy spectrum. There are several processes by which a count may be registered at an energy below the elastic scattering energy. One of the most important of these processes is simply due to the characteristic response of a Si(Li) detector to mono-energetic electrons. An electron incident on the detector may backscatter, not deposit all of its kinetic energy in the detector and thus be counted as a low energy electron. The direct beam curve shows the detector response for our system. This curve was taken with the electron beam directly incident on the detector at zero degrees. This curve provides an indicator of the background to which the inelastic spectra at the various scattering angles must be compared. There can also be a real background from electrons which do not come directly from the target but which have scattered into the collimator system from the chamber walls. We believe this background to be quite small compared to the detector response.

Besides the detector response and the background, there are a number of physical processes which can lead to an electron with an energy less than the incident energy. These are, of course, the processes we are really interested in studying. First, an electron can scatter elastically from an essentially free valence electron in the target. This is the Møller interaction, and although it is kinematically an elastic process, it results in two electrons, each of them with an energy less than the incident kinetic energy. Second, an electron can scatter from an inner shell atomic electron

and excite or ionize the atom. We will be particularly interested in K shell ionization because this process is accompanied by the emission of a characteristic K x-ray by the target atom. Third, the electron can undergo an inelastic scatter from a target atom or electron with the coincident production of a bremsstrahlung photon. Finally, a combination of these processes is possible.

Looking at the data Figures 5 and 6 we can see that the Møller interaction is a dominant feature of the inelastic spectrum. Generally speaking, the Møller interaction results in a peak which moves to lower energy with increasing scattering angle, as expected from kinematics. The cross section for Møller scattering is symmetric about 43 degrees for an incident energy of 120 keV because two scattered electrons result from each interaction. That is, for every electron produced at 30 degrees with an energy of 86 keV there is an electron at 56 degrees with 34 keV. At 20 degrees, the Møller peak is observable at about 105 keV as a shoulder on the low energy side of the Rutherford peak. At 30 degrees, the Møller peak has become quite well resolved at about 86 keV. At 40 degrees, it is still observable at about 65 keV although the cross section is low at this angle. At 60 degrees, the cross section has increased and the peak is observable as an enhancement of counts above the detector noise.

The data at 120 degrees deserves some special attention since the large inelastic spectra can not arise from Møller scattering alone. Kinematically, it is not possible for incident electrons, striking free electrons at rest, to be scattered through an angle greater than 90° . Ford and Mullin² have suggested that there might be multiple processes which could lead to a large inelastic spectrum at backward angles. For example, an incoming electron could scatter first from a loosely-bound valence electron, transferring a substantial fraction of its energy, and then scatter from a nucleus into a backward angle. Figure 7 shows a plot of data taken at a beam energy of 120 keV and scattering angle of 120 degrees from targets

of two different thicknesses. (The data for $200 \mu\text{g}/\text{cm}^2$ is the same as that shown in Figure 6.) If the dominant contribution to the inelastic spectra were from multiple processes, then one might expect that the number of inelastic events relative to Rutherford scattering events would increase with increasing target thickness. To test this dependence on target thickness, measurements were made on targets having thicknesses of 200 and $400 \mu\text{g}/\text{cm}^2$. A non-linear dependence of inelastic events is not at all apparent from the data. If anything, this number seems to decrease slightly with increasing target thickness. The data at $400 \mu\text{g}/\text{cm}^2$ and 120 degrees was taken in a single run immediately following the run at $200 \mu\text{g}/\text{cm}^2$. The beam conditions were not changed, the only change was the raising of the appropriate target into the beam. Clearly, additional measurements are necessary to understand this effect at backward angles.

In the inelastic spectra, some electrons no doubt arise from K shell ionization and bremsstrahlung interactions. These processes cannot easily be separated from the total spectra because the cross sections are low and because the electron energy is not fixed by kinematics for a fixed scattering angle as it is in the Møller and Rutherford interactions. The study of these processes is, of course, the motivation for the coincidence experiments. By looking at the K x-ray or bremsstrahlung photon in time coincidence with the scattered electron, these inelastic processes can be separated and their differential cross sections measured.

Figure 8 shows some data taken at an incident energy of 140 keV. Again, the Møller peak at 30 degrees and 101 keV is well resolved. Figure 9 shows a comparison of data taken at 140 keV at 30 degrees with targets of $400 \mu\text{g}/\text{cm}^2$ and $200 \mu\text{g}/\text{cm}^2$ thickness. The Rutherford peak is slightly broader with the thicker target. Thinner targets were not available when these data were taken, but we have since succeeded in fabricating some self-supporting aluminum targets of $100 \mu\text{g}/\text{cm}^2$ thickness. The Møller peak is almost completely

washed out with the thicker target. This we believe is due to the spread in energy of a Møller scattered electron caused by attenuation in the target. The resolution of the Møller peak is also sensitive to the angular resolution of the collimator system. Figure 10 shows data at 30 degrees and 120 keV from a $200 \mu\text{gm}/\text{cm}^2$ aluminum target with less collimation on the detector. The data in Figure 10 should be compared with corresponding data in Figure 5. The latter data as well as that shown in Figures 6 - 9 was taken with the smallest collimator used. It consisted of two 0.031 inch aluminum apertures separated by 2.5 inch. The data in Figure 10 was taken with a larger collimator consisting of a front aperture of 0.187 inch and a rear aperture of 0.062 inch separated by 2.5 inch. We see that for the large collimator, that is, for poorer angular resolution of the scattered beam, the Møller peak is washed out somewhat with the excess counts at higher energy. Again, we believe this is due to the spread in energy that results when the scattering angle is not precisely defined.

This investigation has been very useful as a necessary step to the coincidence measurements. We have learned how well we must focus and collimate the incident beam. We have learned how well the detector must be collimated and shielded in order that the spread in energy that results with angular spread in the inelastic processes not be too serious. The study has raised some interesting questions in itself. The backward angle spectra is not understood. It would be interesting to make more measurements with thinner aluminum targets and perhaps investigate the spectra from tin and gold targets as well. We hope to continue to pursue these measurements during the next year.

Some of these results were reported in a paper presented at the Texas Academy of Science Meeting, March 13-15, 1969.

2. Coincidence experiments.

It was initially felt that a study of the K ionization process

would provide a good check out for the bremsstrahlung-electron coincidence measurements. It has now become quite apparent that the study of the electron angular distribution in coincidence with K shell ionization is very important in its own right, and such a study will form the topic of a doctoral dissertation of one of the graduate students involved in the project. Most of our studies so far have been made at an electron energy of 120 keV with an $80 \mu\text{gm}/\text{cm}^2$ tin target. A block diagram of the electronics is shown in Figure 4.

For the initial tests, the photon detector has been set at 135 degrees to the incident beam. The electron detector has been set around 40 degrees. Since the K x-rays accompanying the ionization interactions are isotropic, the 135 degree angle was chosen in order to minimize the bremsstrahlung from the target. (To look directly for bremsstrahlung coincidence events, the photon detector should be moved to a forward angle, of course.) At first, the largest background in the photon detector was due to electrons which backscattered from the target, hit the detector and produced thick target bremsstrahlung in the beryllium window of the detector. In order to eliminate this background, a small horseshoe magnet with a field of about 500 gauss was enclosed in magnetic shielding material and placed just outside the brass collimator on the photon detector. The backscattered electrons are bent in this field and completely miss the detector window. Figure 11 shows a photon spectrum without the magnet and Figure 12 shows a spectrum taken with the magnet in place. The improvement is by a factor of about 30. The K_α and K_β characteristic x-rays from the tin target are very well resolved.

Coincidence measurements have been made using an open Cerium 139 source mounted in the scattering chamber at the target position. Cerium 139 has a K-shell conversion electron of 126.9 keV energy accompanied by a characteristic K x-ray from Lanthanum of 33.2 keV. While the source is quite weak and the coincidence rate very low,

this measurement does allow us to thoroughly check out the electronics and to precisely set the timing of the coincidence channels.

After installing the magnet on the photon detector, some coincidence measurements were made with an essentially uncollimated electron detector to investigate the accidental coincidence problem. These measurements were made with a coincidence circuit which was not capable of better than about 100 nsec resolution. The result, as expected, was that most coincidence events were accidental. Since these measurements, we have been attacking the accidental coincidence problem on two fronts. First, we have just received and tested a new version of the coincidence circuit which is capable of about 5 nsec ultimate resolution. With our detectors and their intrinsic time jitter we should easily be able to achieve about 20 nsec resolution and perhaps 10 nsec with some effort. The addition of this circuit alone will, of course reduce the accidental rate by a factor of about 5.

Second, one has only to look at Figures 5 - 10 to observe a major source of accidental coincidences. With the electron detector at 30 degrees and the single channel analyzer set to span the inelastic energy range, we see that the bulk of the counts would arise from the detector response to the Rutherford peak. That is, if all electrons scattered at 30 degrees are allowed to hit the detector, the vast majority of these are Rutherford scattered. Although we can exclude from coincidence those electrons in the Rutherford peak itself, we cannot exclude those electrons which fall into the inelastic region as a result of backscatter from the detector. It is vitally important, then, to prevent those electrons which have Rutherford scattered from hitting the detector. To this end, we have devoted some effort to designing and testing a spectrometer.

What we need, ideally, is a device which will allow us to exclude the Rutherford peak and yet detect the entire inelastic energy region. We must be able to mount the device in the scattering

chamber on the rotatable arm. We have built and are testing an electrostatic spectrometer. The major advantage of such an electrostatic instrument is that the energy region accepted can be easily varied by changing the electric field and that the shielding of the beam from the device is not difficult. A schematic diagram of the spectrometer is shown in Figure 13. A disadvantage, curiously enough, is that the energy resolution is much too good for our application. Figure 14 shows a plot of intensity versus spectrometer voltage (or electron energy). These data were taken using two sources of mono-energetic electrons: cerium 139 and gold 195. There was essentially no collimator at the entrance to the spectrometer so these data represent about the broadest acceptance one could expect from the instrument. The data points represent the result of summing the counts under the full energy peak and subtracting a background for each setting of the voltage on the spectrometer. This spectrometer, while not so useful for the K ionization measurement, should be very useful in the bremsstrahlung measurements where one can fix the electron energy and observe the bremsstrahlung energy spectrum.

We felt that the resolution problem might be solved most quickly for the K ionization measurements by designing a magnetic spectrometer with specially shaped pole faces to enable us to accept electrons with energies between about 40 and 100 keV. A schematic diagram of this spectrometer is shown in Figure 15. The field is provided by a small horseshoe magnet. The pole faces are separated by 0.2 in. and the field inside is quite uniform and about 620 gauss. The detector is placed so as to intercept the electrons with energies between 40 and 100 keV. We are still in the process of testing and refining this spectrometer.

We believe that the improved coincident circuit coupled with the elimination of the Rutherford scattered electron should reduce the accidental problem to a quite acceptable level. At this point we are very hopeful of having angular distributions of electron in

coincidence with K x-rays from tin and some initial angular distributions in coincidence with bremsstrahlung by the end of the summer.

III. PERSONNEL

One of the important indirect aims of this research program is the training of graduate students. During the course of this contract period, four graduate students have worked on the project. Mr. Doyle Davis has been a NASA Trainee and is expected to complete his Ph.D. degree during the coming year. The studies of K x-rays in coincidence with inelastically scattered electrons should form the subject of his dissertation. Mr. David Heroy has held an NDEA Fellowship. It is expected that the subject of his dissertation will be the bremsstrahlung-electron coincidence studies. In addition to these two full time students, two other graduate students have been associated with the project part time. Mr. George Mak worked full time from February to June, completed an M.S. degree and has taken a job in industry. Mr. Jerry Faulk has worked with us two months this summer and will return to a high school teaching job next year before continuing his graduate studies.

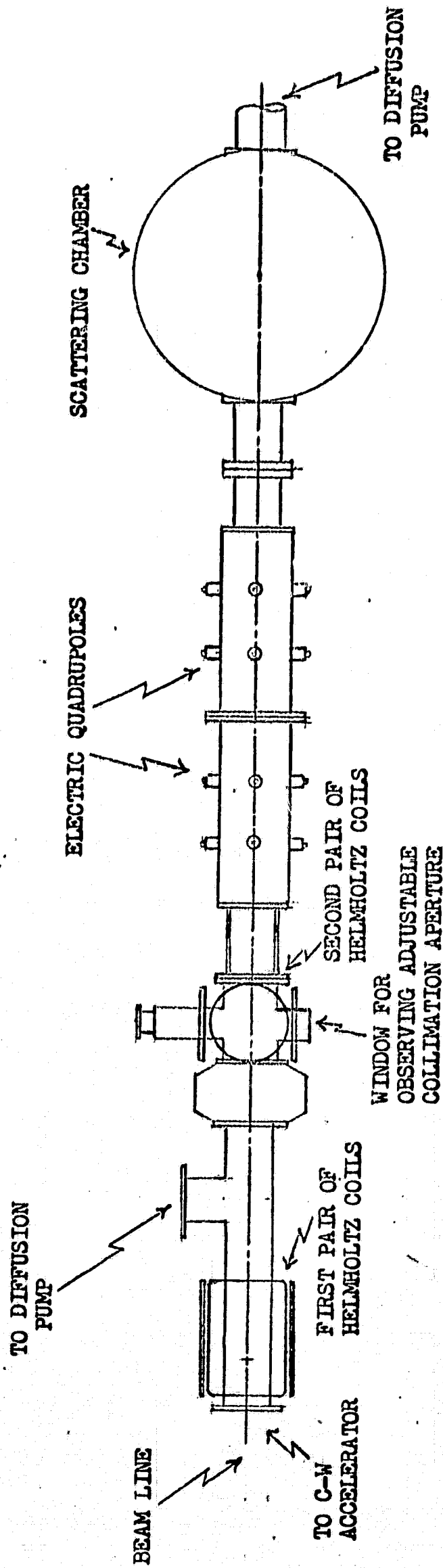
During the past year, five undergraduate students have been associated with the laboratory for various periods of time and have participated in several aspects of the research program.

REFERENCES

- ¹C. E. Dick and J. W. Motz, Physical Review 171, 75 (1968).
- ²C. W. Ford and C. J. Mullin, Physical Review 110, 520 (1958).

FIGURE CAPTIONS.

1. Beam layout showing steering coils, focussing quadrupoles and scattering chamber.
2. Plan view of the scattering chamber.
3. Side view of the scattering chamber with the Ge(Li) detector installed in the top.
4. Block diagram of the electronics used for coincidence measurements. Delay amplifiers are not shown.
5. Total inelastic spectra at 20° and 30° for 120 keV electron on 200 $\mu\text{gm}/\text{cm}^2$ aluminum.
6. Total inelastic spectra at 40°, 60° and 120° for 120 keV electrons on 200 $\mu\text{gm}/\text{cm}^2$ aluminum.
7. Total inelastic spectra at 120° for 120 keV electron on 200 $\mu\text{gm}/\text{cm}^2$ and 400 $\mu\text{gm}/\text{cm}^2$ aluminum targets.
8. Total inelastic spectra at 30° and 60° for 140 keV electron on 200 $\mu\text{gm}/\text{cm}^2$ aluminum.
9. Total inelastic spectra at 30° for 140 keV electrons on 200 $\mu\text{gm}/\text{cm}^2$ and 400 $\mu\text{gm}/\text{cm}^2$ aluminum targets.
10. Total inelastic spectrum at 30° for 120 keV electrons on 200 $\mu\text{gm}/\text{cm}^2$ aluminum taken with large collimator (poorer angular resolution).
11. Characteristic K x-ray spectrum at 135° from an 80 $\mu\text{gm}/\text{cm}^2$ tin target bombarded with 120 keV electrons. This spectrum was taken before the magnet was installed in front of the Ge(Li) detector.
12. Same as Figure 11, but after the magnet was installed.
13. Schematic of the electrostatic spectrometer.
14. Intensity versus spectrometer voltage (or electron energy) for monoenergetic electrons incident on the electrostatic spectrometer.
15. Schematic of the magnetic spectrometer.



BEAM LAYOUT
TOP VIEW

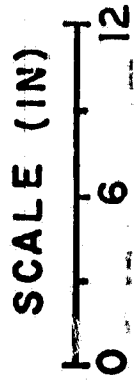
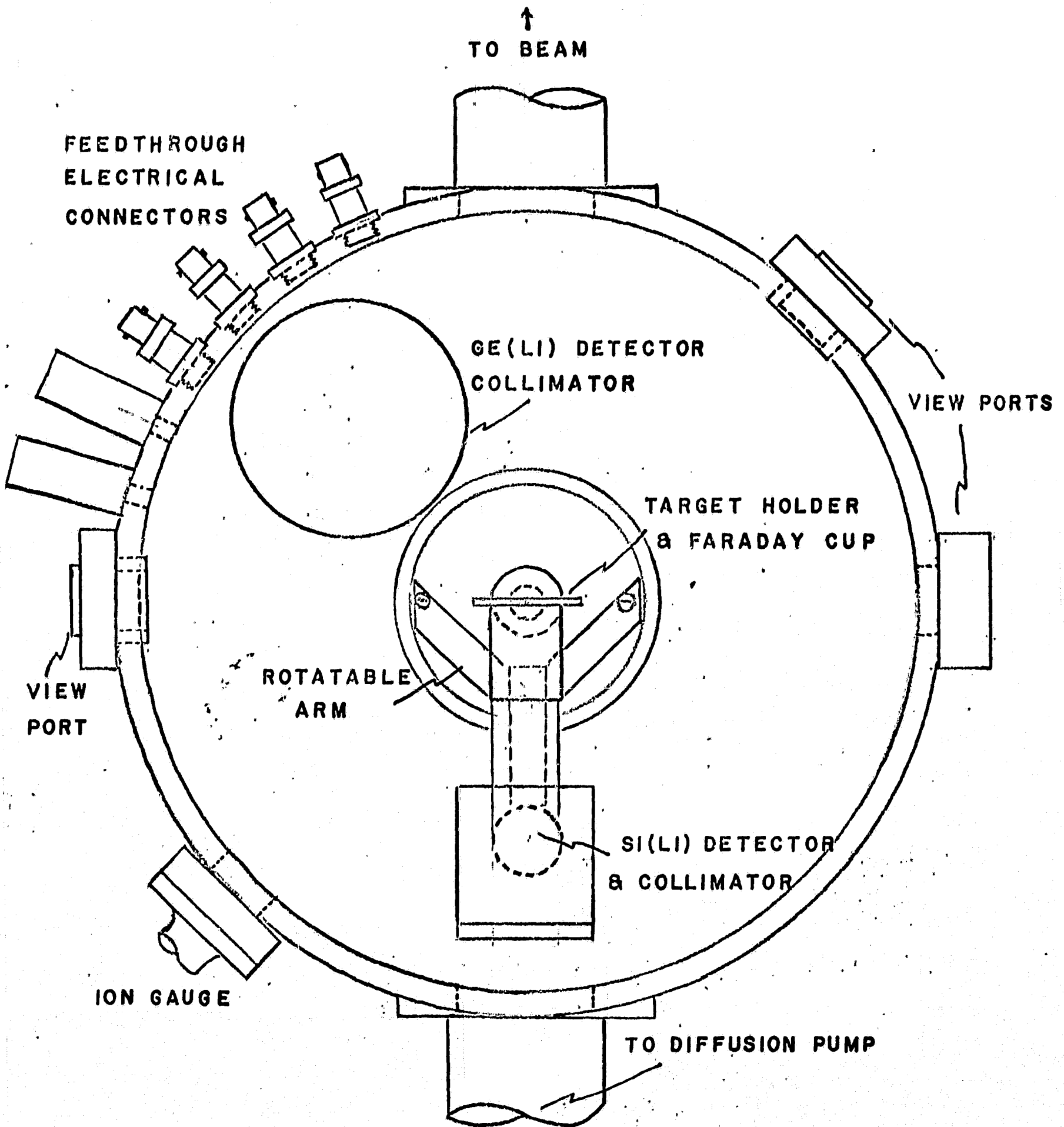
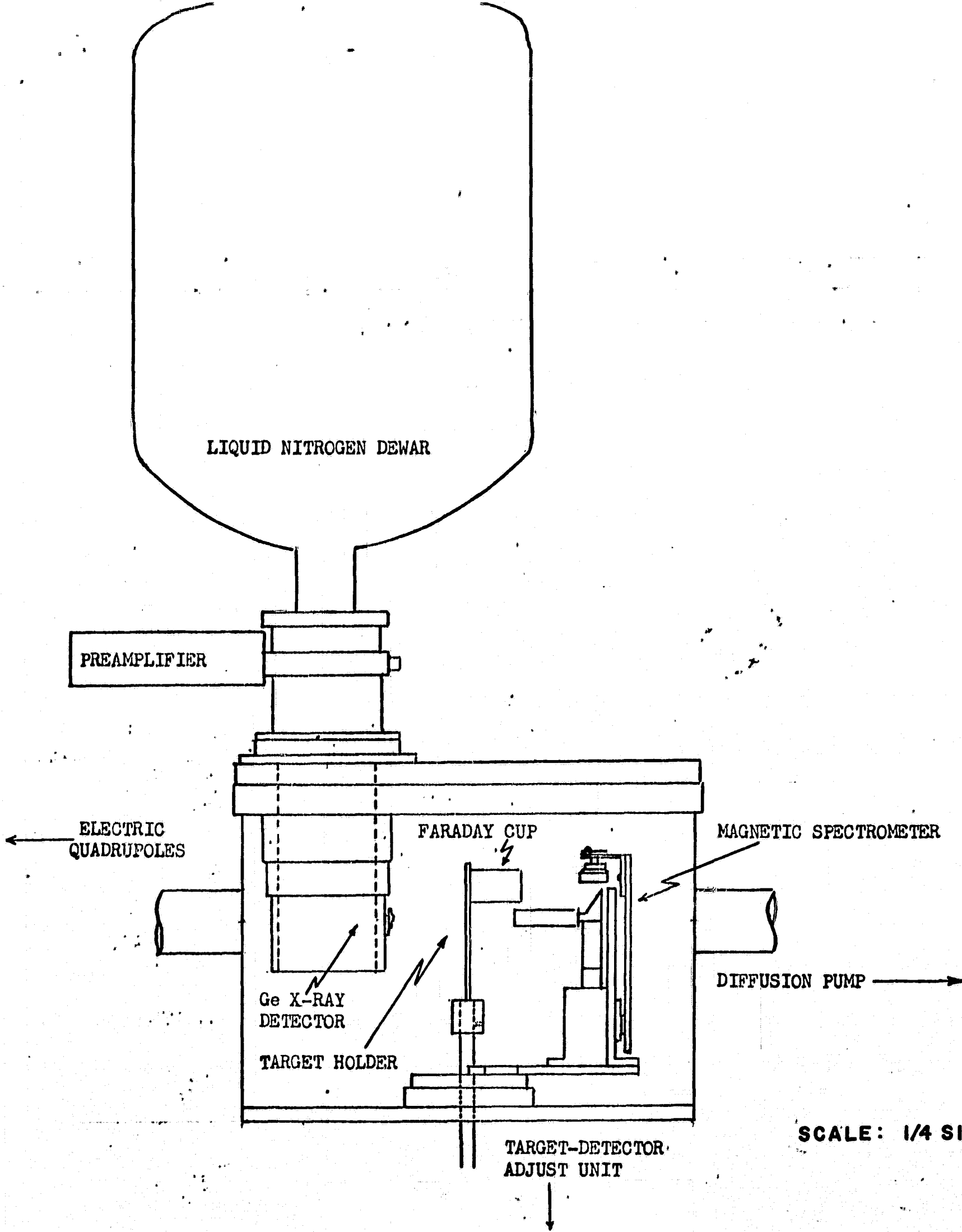


FIG. 1



SCATTERING CHAMBER
(ACTUAL SIZE)

FIG. 2

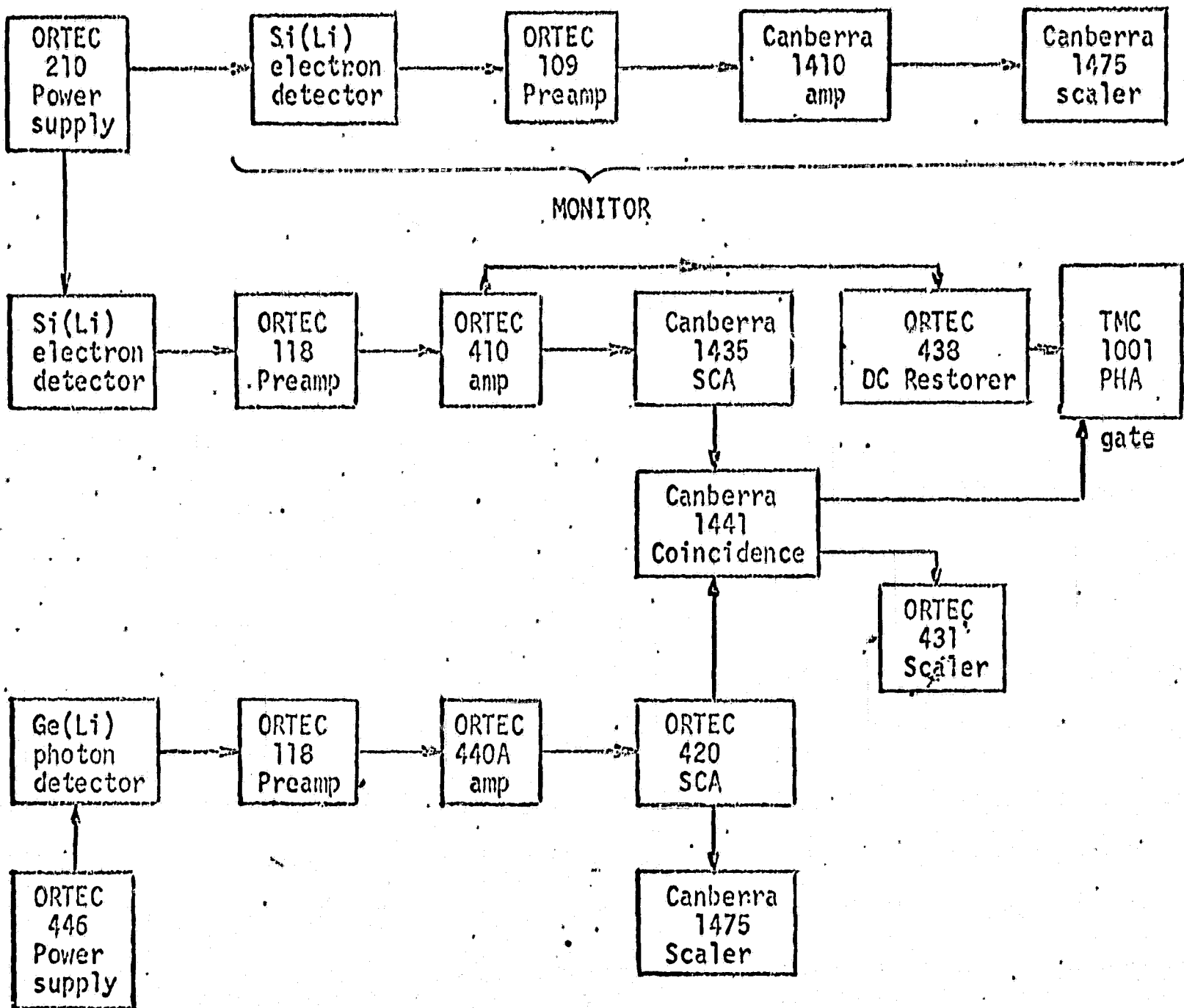


SCALE: 1/4 SIZE

SCATTERING CHAMBER

(SIDE VIEW)

FIG. 3



BLOCK DIAGRAM FOR
COINCIDENCE EXPERIMENTS

FIG. 4

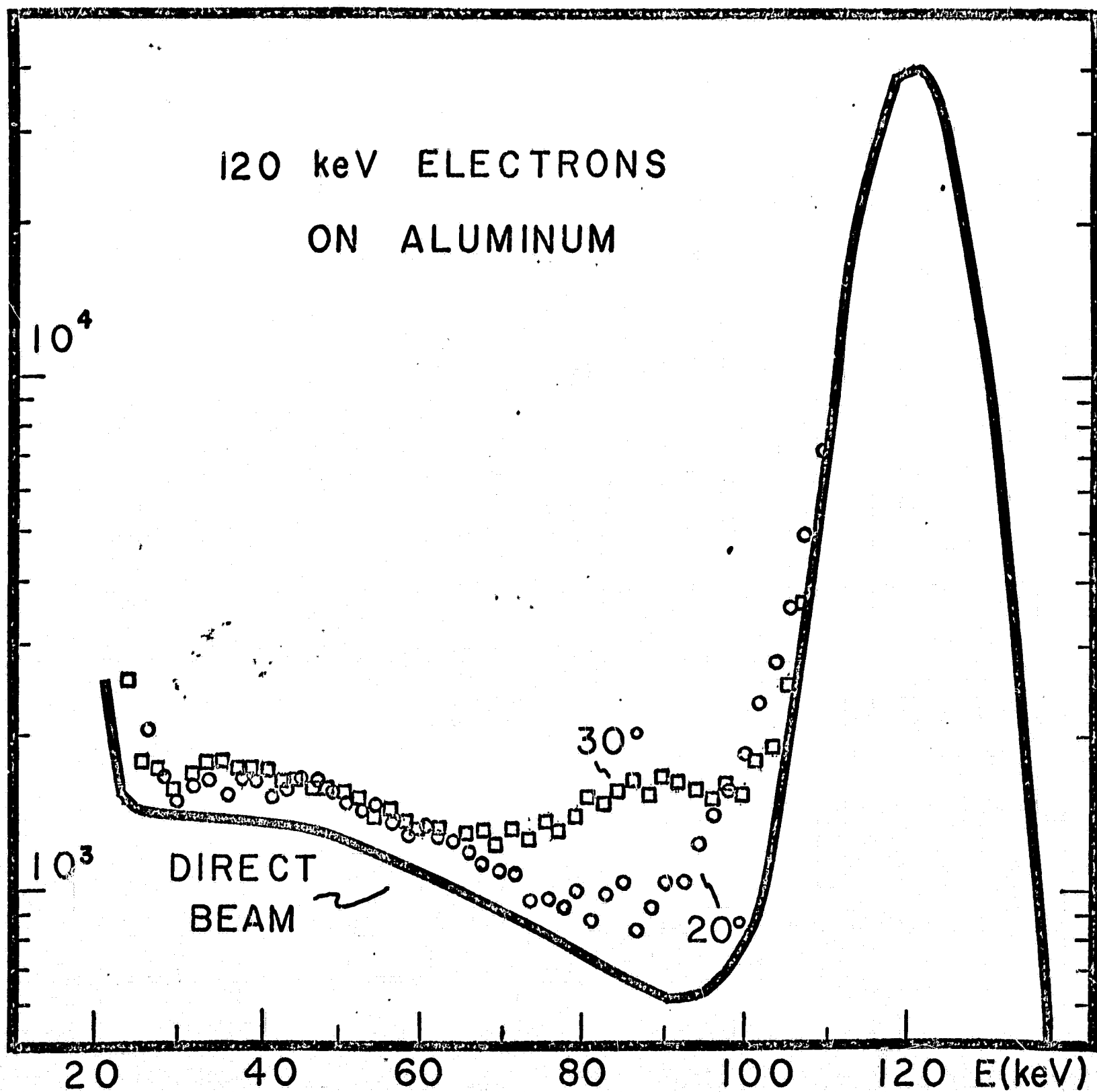


FIG. 5

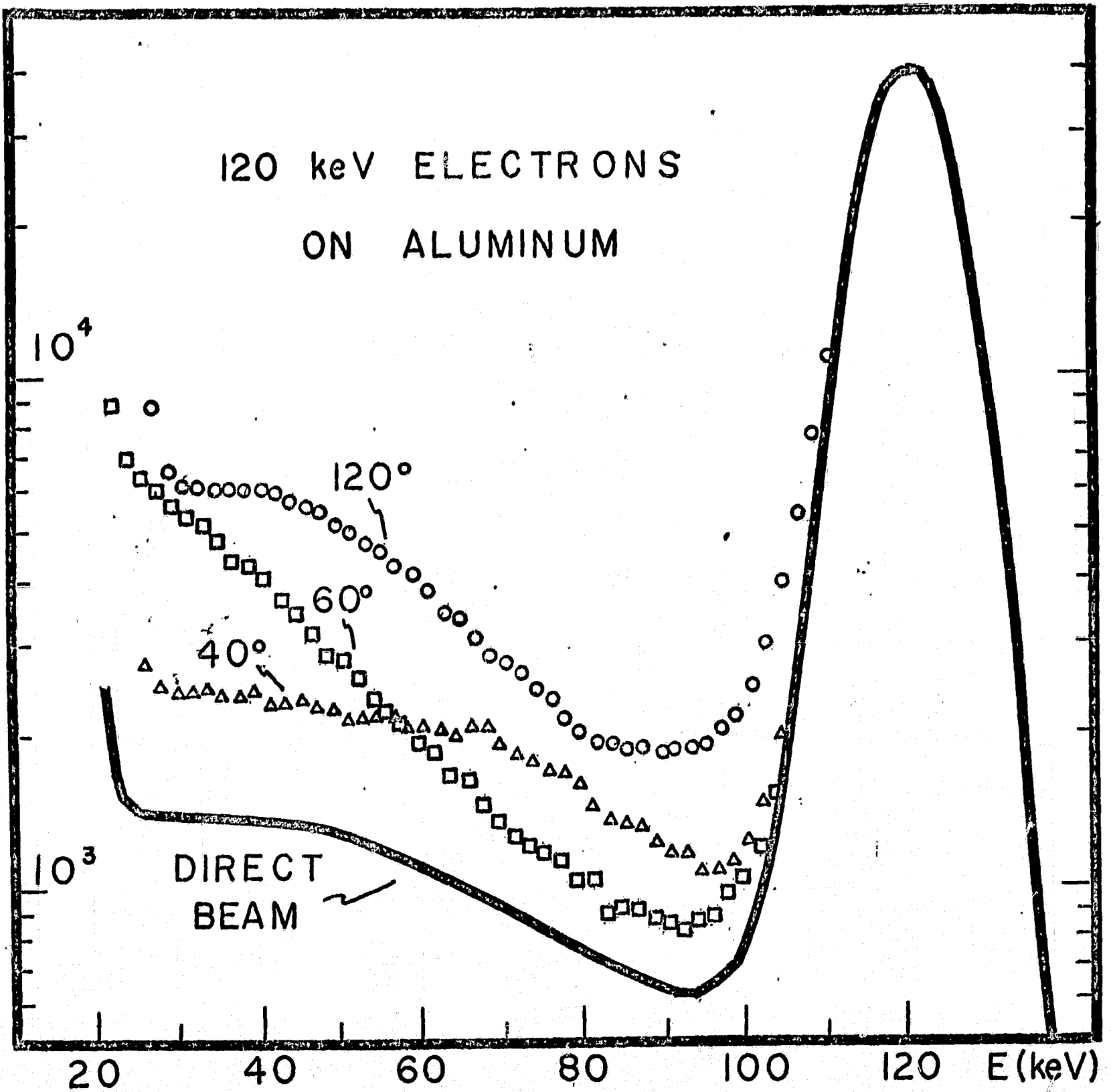


FIG. 6

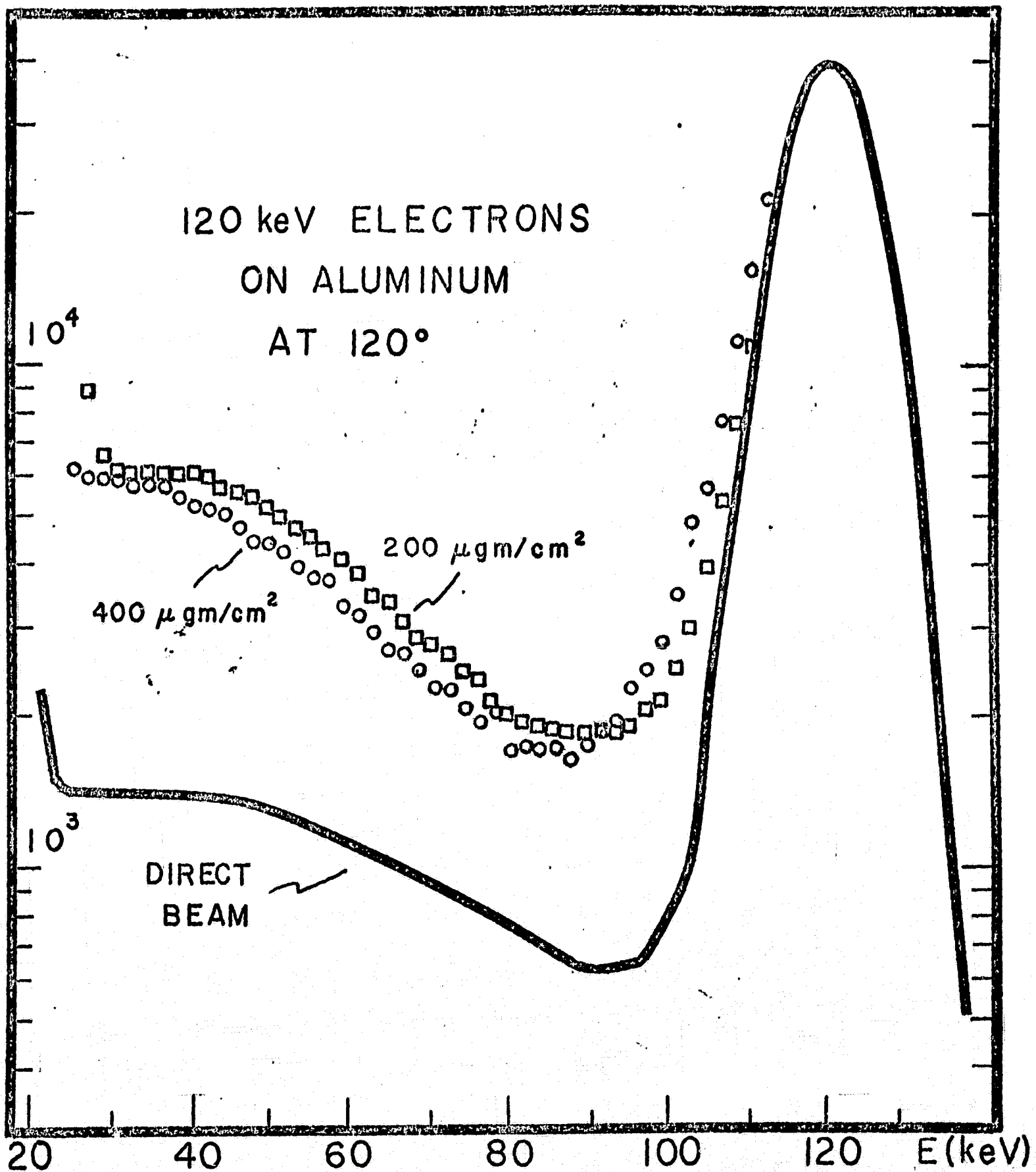


FIG. 7

140 keV ELECTRONS ON ALUMINUM

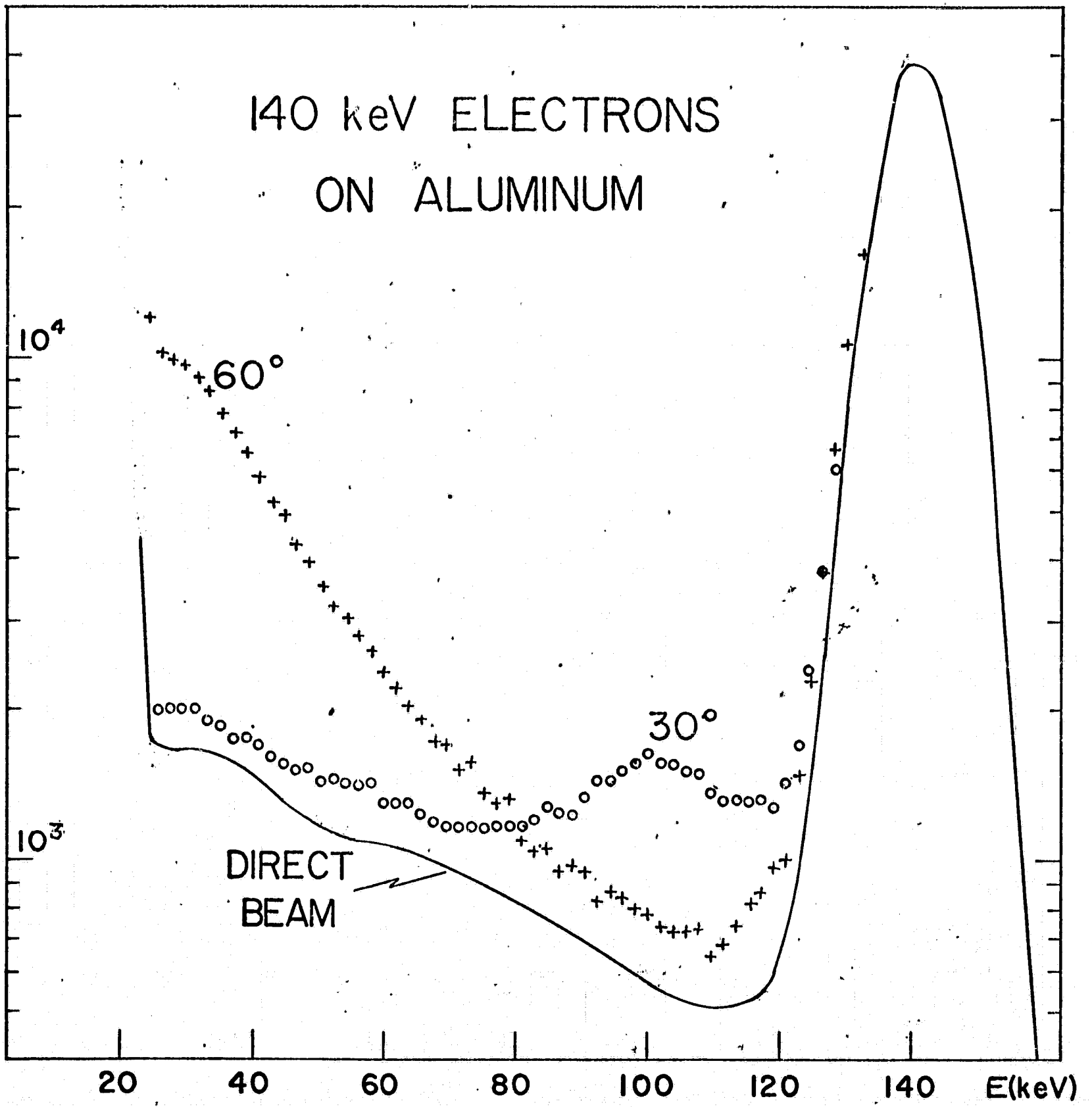


FIG. 8

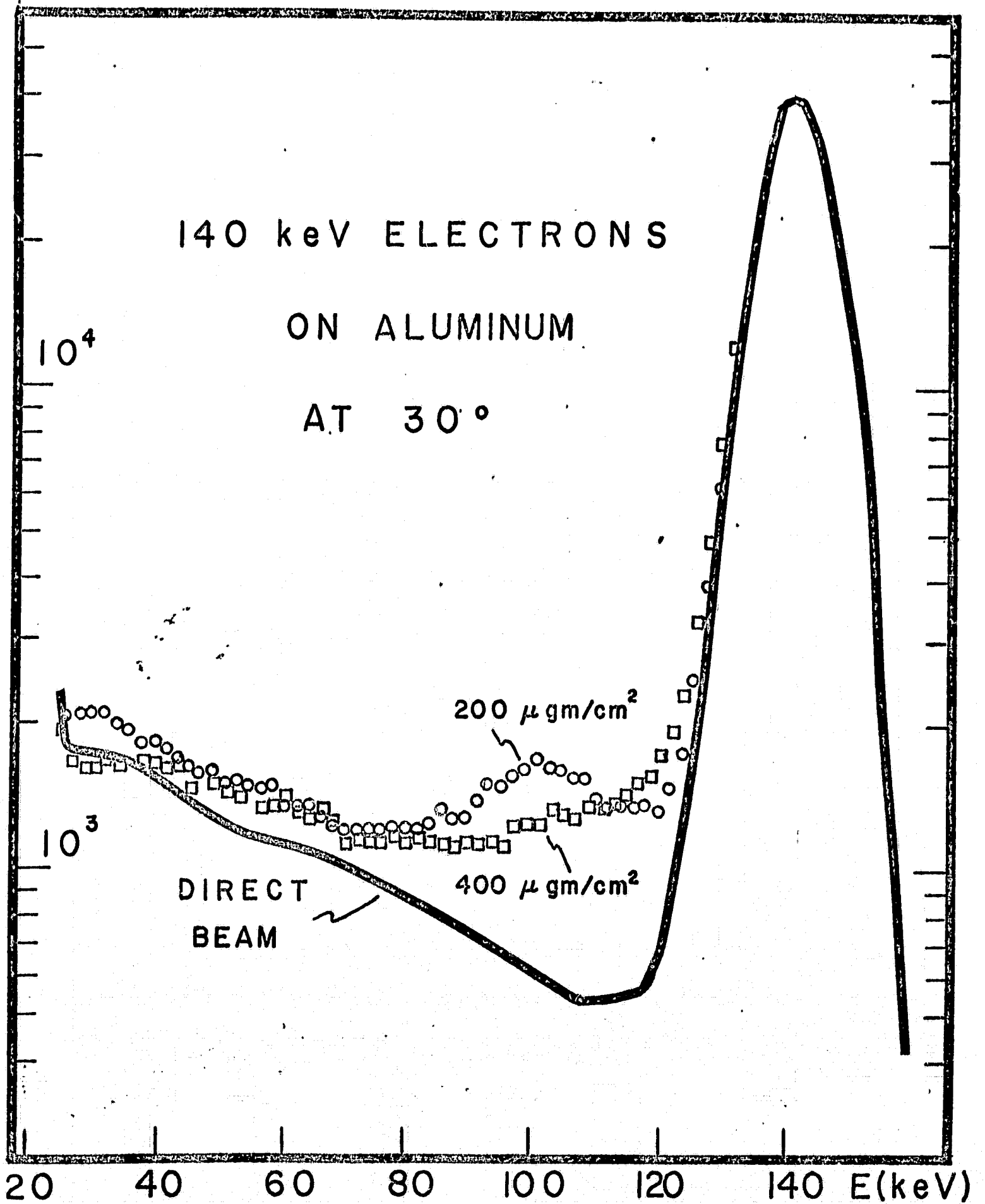


FIG. 9

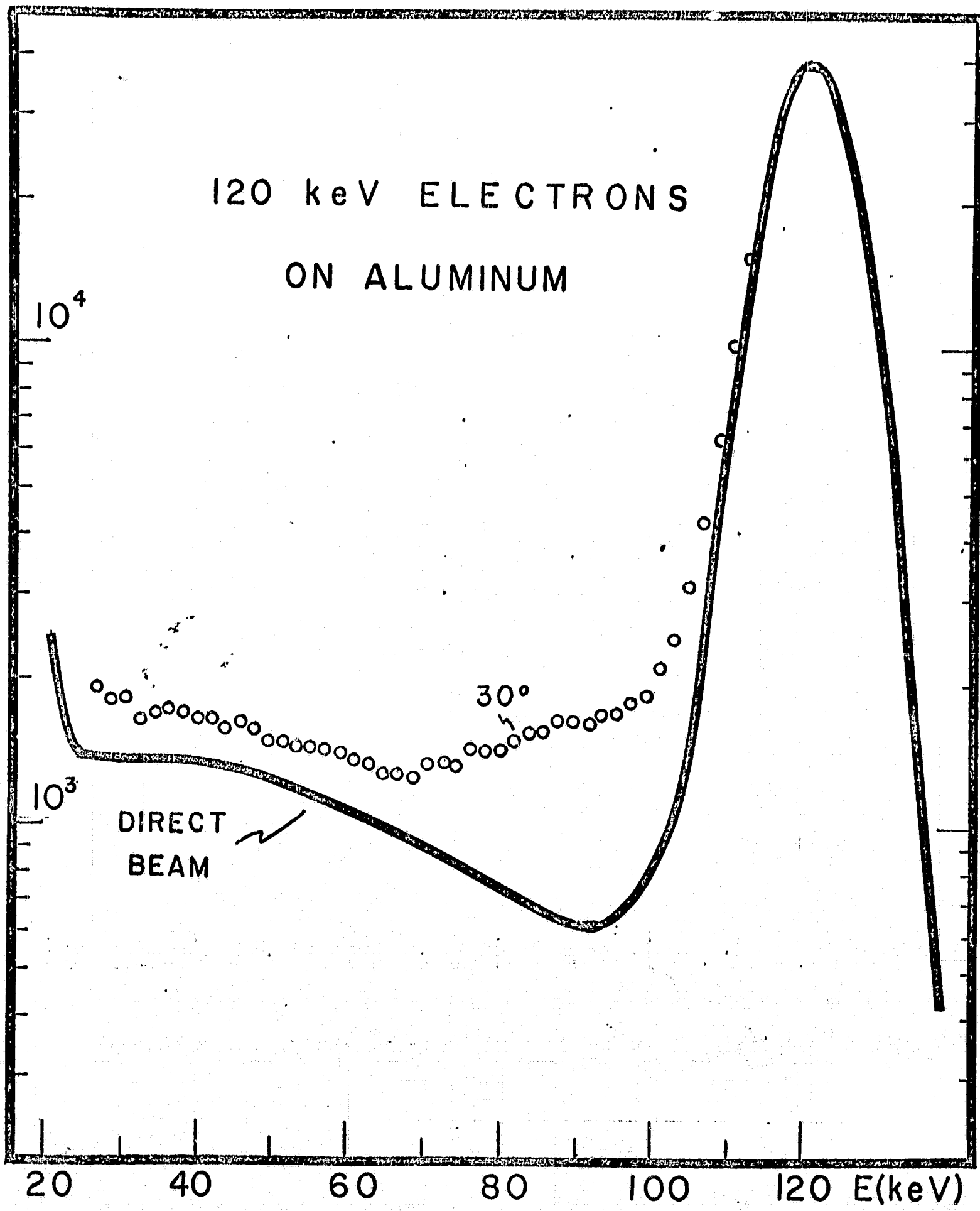


FIG. 10

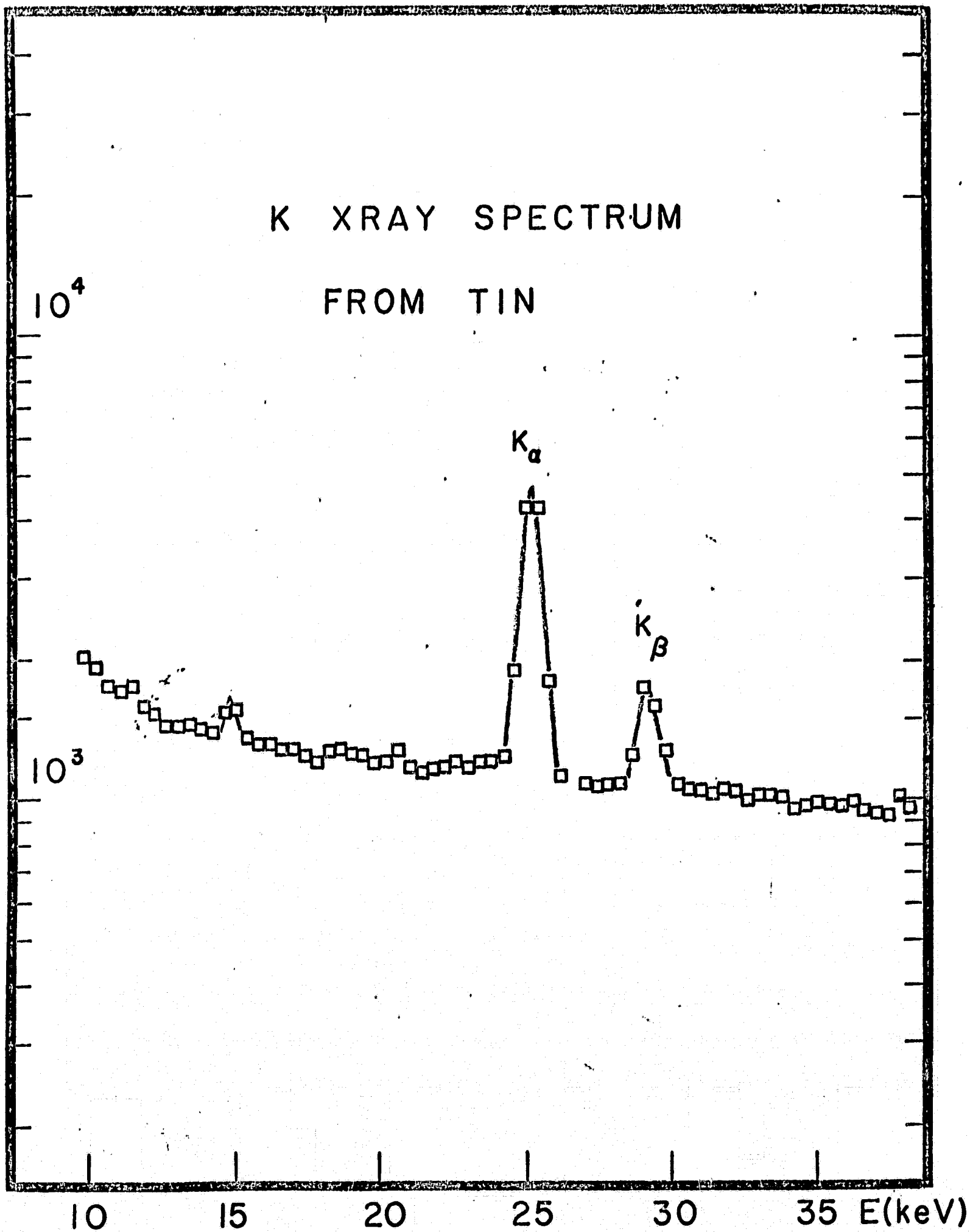


FIG. II

K XRAY SPECTRUM

FROM TIN

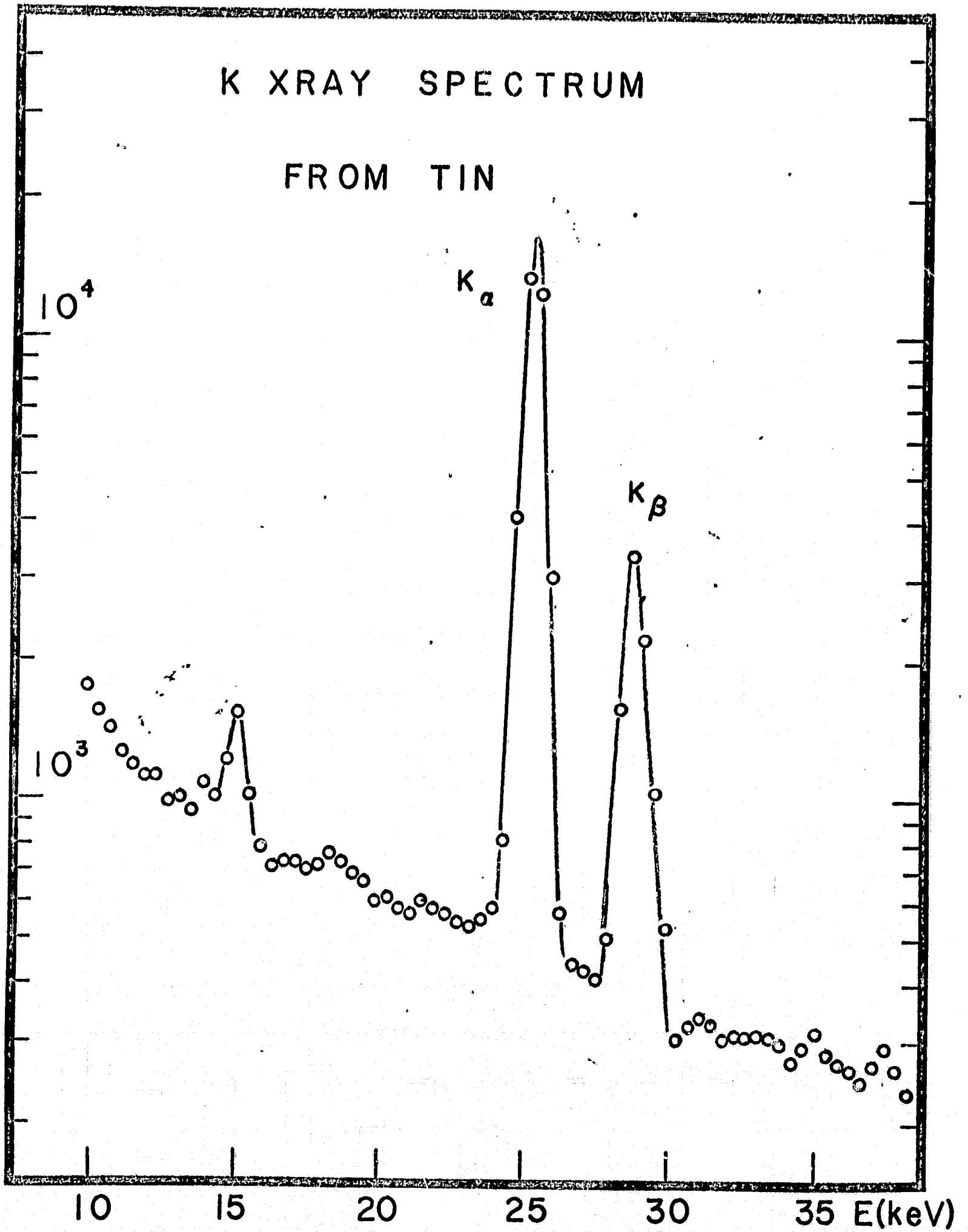
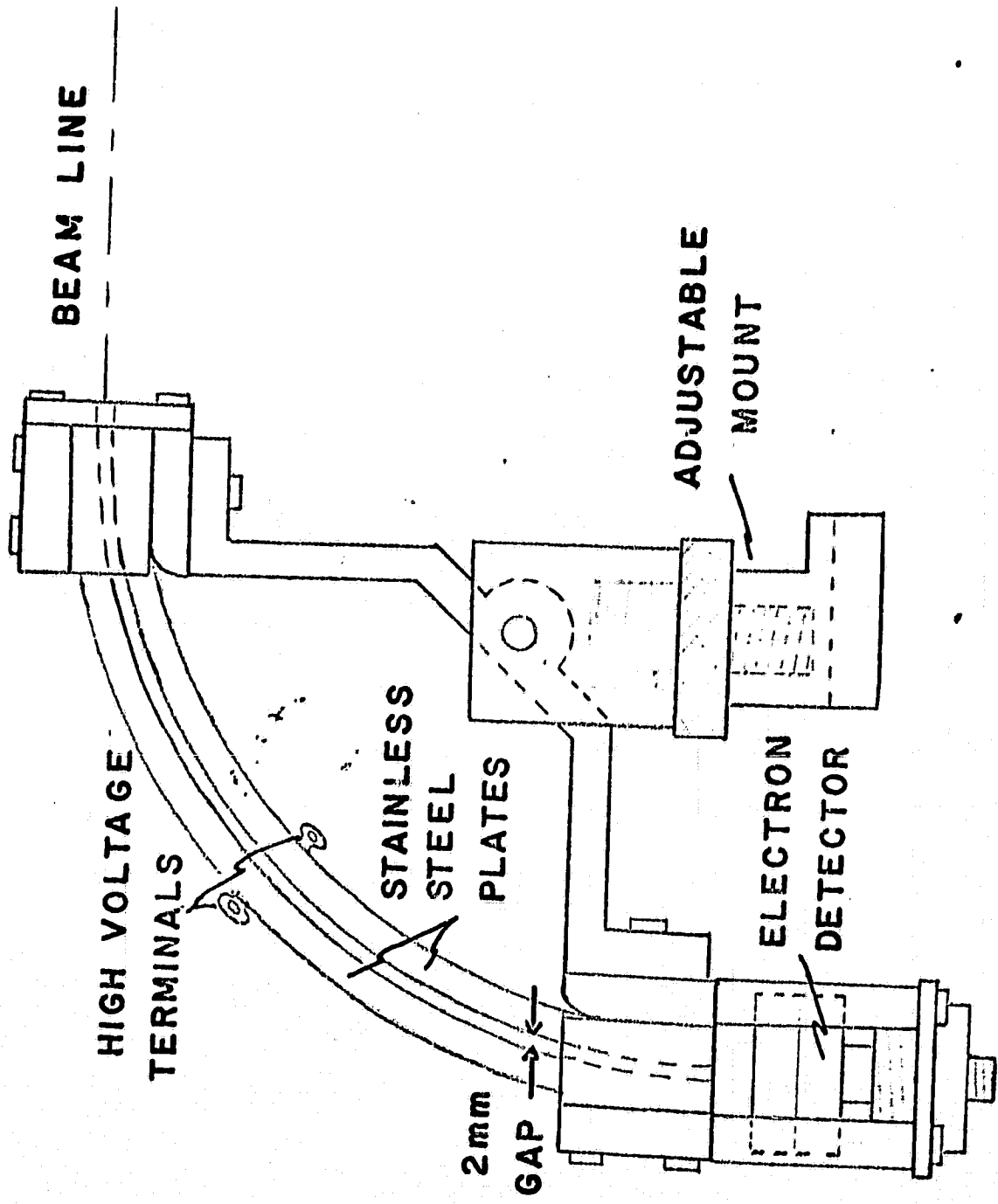


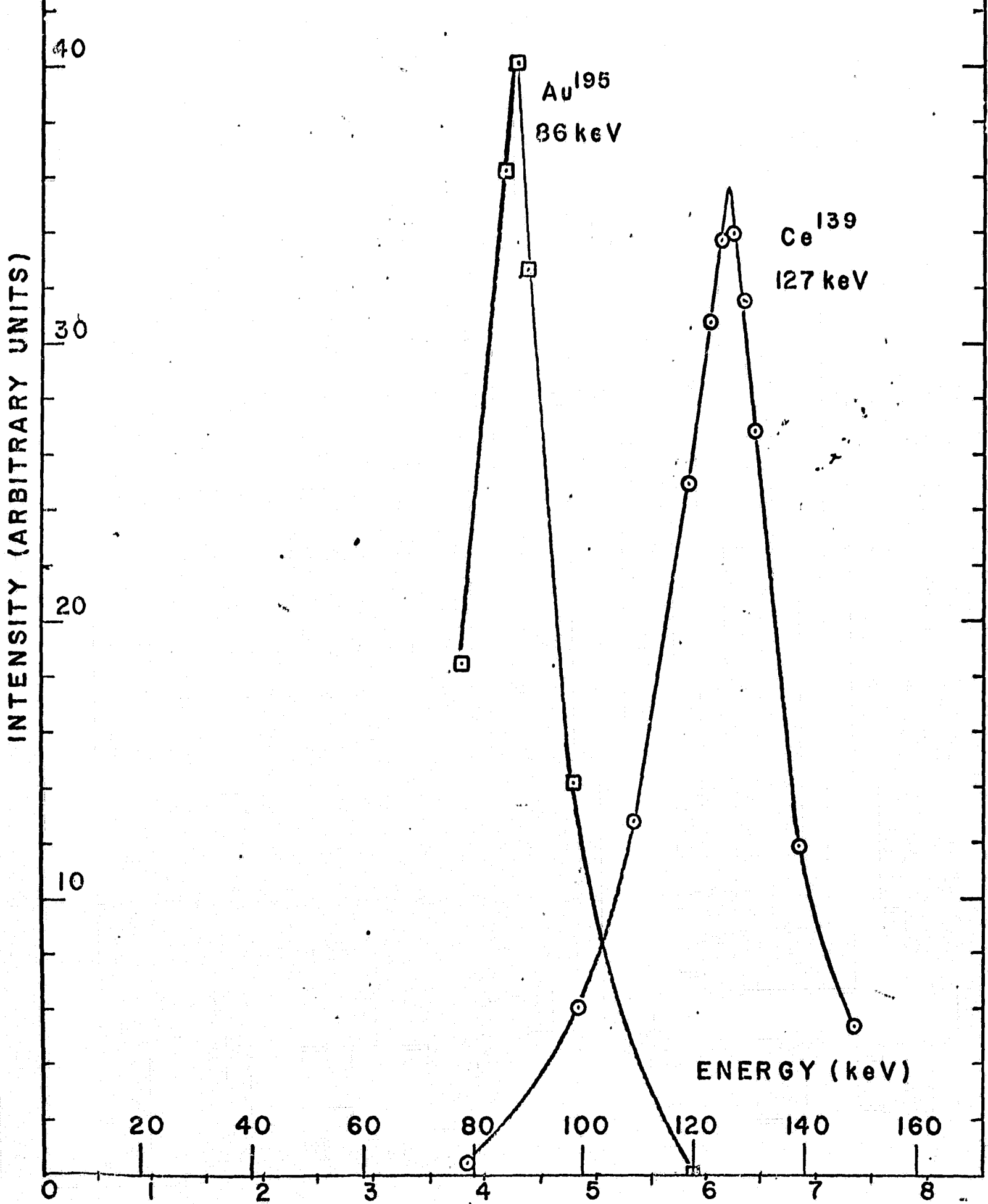
FIG. 12



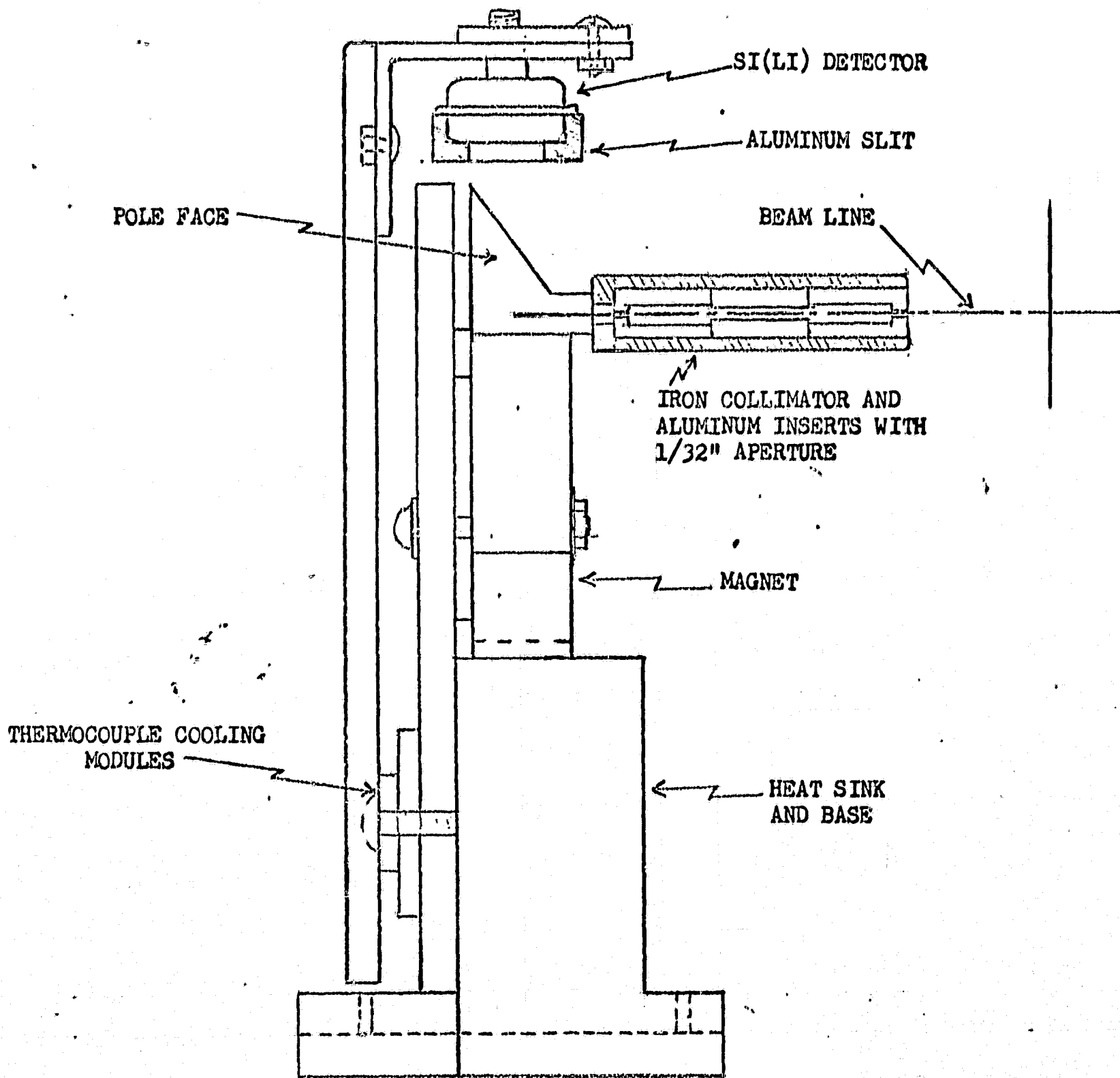
ELECTROSTATIC SPECTROMETER
(ACTUAL SIZE)

FIG. 13

INTENSITY VERSUS VOLTAGE
FOR MONO-ENERGETIC ELECTRONS



VOLTAGE (KILOVOLTS) FIG. 14



MAGNETIC SPECTROMETER

(ACTUAL SIZE)

FIG. 15